CrossMark

EFFECT-RELATED EVALUATION OF ANTHROPOGENIC TRACE SUBSTANCES, -CONCEPTS FOR GENOTOXICITY, NEUROTOXICITY AND, ENDOCRINE EFFECTS

Fishing for contaminants: identification of three mechanism specific transcriptome signatures using *Danio rerio* embryos

Jonas Hausen[1] · Jens C. Otte[2] · Jessica Legradi[3] · Lixin Yang[2] · Uwe Strähle[2] ·
Martina Fenske[4] · Markus Hecker[5] · Song Tang[5] · Monika Hammers-Wirtz[6] ·
Henner Hollert[1] · Steffen H. Keiter[1,7] · Richard Ottermanns[1]

Abstract In ecotoxicology, transcriptomics is an effective way to detect gene expression changes in response to environmental pollutants. Such changes can be used to identify contaminants or contaminant classes and can be applied as early warning signals for pollution. To do so, it is important to distinguish contaminant-specific transcriptomic changes from genetic alterations due to general stress. Here we present a first step in the identification of contaminant class-specific transcriptome signatures. Embryos of zebrafish (*Danio rerio*) were exposed to three substances (methylmercury, chlorpyrifos and Aroclor 1254, each from 24 to 48 hpf exposed) representing sediment typical contaminant classes. We analyzed the altered transcriptome to detect discriminative genes significantly regulated in reaction to the three applied contaminants. By comparison of the results of the three contaminants, we identified transcriptome signatures and biologically important pathways (using Cytoscape/ClueGO software) that react significantly to the contaminant classes. This approach increases the chance of finding genes that play an important role in contaminant class-specific pathways rather than more general processes.

✉ Jonas Hausen
jhausen@bio5.rwth-aachen.de

[1] Institute for Environmental Research, RWTH Aachen University, Worringerweg 1, 52074 Aachen, Germany

[2] Institute of Toxicology and Genetics, Karlsruhe Institute of Technology, Hermann-von-Helmholtz-Platz 1, 76344 Eggenstein-Leopoldshafen, Germany

[3] Environment and Health, VU Amsterdam, De Boelelaan 1087, 1081 HV Amsterdam, the Netherlands

[4] Fraunhofer Institute for Molecular Biology and Applied Ecology IME, Project Group for Translational Medicine and Pharmacology, Forckenbeckstraße 6, 52074 Aachen, Germany

[5] School of Environment and Sustainability, University of Saskatchewan, Saskatoon, SK S7N 5C8, Canada

[6] Research Institute for Ecosystem Analysis and Assessment - gaiac, Kackertstraße 10, 52072 Aachen, Germany

[7] Man-Technology-Environment Research Centre, Örebro University, SE-701 82 Örebro, Sweden

Introduction

In environmental sciences, transcriptomic techniques like microarrays allow a comprehensive analysis of an organism's molecular response to contaminant exposure, diseases, and changes in the external environment. Enabling the study of large numbers of genes at the same time, these methods have become powerful tools for transcriptome profiling and led to the development of (eco)toxicogenomics (Snape et al. 2004; Lettieri 2006; Fedorenkova and Vonk 2010). Snell et al. (2003) pointed out that one way to advance ecotoxicogenomics is to detect certain genes that are significantly regulated in response to contaminant exposure, characterize those genes, and use them to identify stressors.

Springer

At present, only a few existing bioassays on aquatic organisms are able to measure molecular or mechanism-specific effects and to display bioavailable hazard potential of pollutants (Hollert et al. 2003; Schiwy et al. 2014; Garcia-Käufer et al. 2015). Zebrafish (*Danio rerio*) is increasingly used in ecotoxicological screening and profiling (Höss et al. 2010; Feiler et al. 2013) and represents a prominent and genetically well-characterized organism. In addition, zebrafish is one of only a few fish species whose genomes are sequenced and publically available and whose gene functions are well known due to a large number of experimental studies on gene knockout and expression profiles (Van Aggelen et al. 2010; Howe et al. 2013). Thus, the usage of *D. rerio* transcriptomics in ecotoxicological studies can provide information regarding the genetic regulation and adaptation of this organism exposed to changing environmental conditions (Keiter et al. 2010; Braunbeck et al. 2015).

It was already shown that certain contaminants cause barcode-like responses on transcriptome level, which can be used to distinguish between these substances (Lettieri 2006; Yang et al. 2007). Specific genes or transcriptome signatures are claimed to be used as early warning signals for pollution (Bartosiewicz et al. 2001; Snell et al. 2003; Fedorenkova and Vonk 2010). However, previous studies using microarrays to examine the effects of contaminant exposure on an organism were mostly conducted on single substances. This limits the explanatory power because it is hard to distinguish genes or pathways that react specifically to the tested components from those involved in general stress responses or systemic toxicity (Kosmehl et al. 2012). The latter can be expected to react to any kind of contaminant and are therefore not suitable for an identification of contaminant class-specific mechanisms.

The aim of this study was to find variations in gene expression of zebrafish embryos after exposure to different contaminant classes and to identify specific transcriptome signatures. Detecting genes and pathways that reliably identify contaminant classes is instrumental for a successful integration of ecotoxicogenomics into ecotoxicology. In addition, this can be a starting point for the investigation of molecular mechanisms and the definition of modes of action of environmental contaminations.

We conducted a comparison of the gene expression profiles for three relevant contaminants. Thus, we performed transcriptome analyses with zebrafish embryos to identify genes and pathways expressed significantly different for each contaminant. The transcriptome was analyzed after 48 h post-fertilization (hpf) exposure to three model compounds (chlorpyrifos, methylmercury, and Aroclor 1254 as a technical PCB mixture), which had been selected as representatives of common classes of environmental contaminants. Particularly, they can be found in aquatic sediments where they cause specific effects in aquatic organisms. Methylmercury was selected as a representative of heavy metals. Methylmercury exposure has been shown to cause various cellular changes including lipid peroxidation, DNA damage, membrane structure alteration, mitochondrial dysfunction, cell cycle alteration, apoptosis, and necrosis (Clarkson and Magos 2006). Chlorpyrifos belongs to the group of organophosphate pesticides, which are widely used in agriculture today (Uzun and Kalender 2013). Both methylmercury and chlorpyrifos are known to cause neurotoxic effects in zebrafish (Whitney et al. 1995; Hassan et al. 2012; Ho et al. 2013). Aroclor 1254 is a mixture of polychlorinated biphenyls and represented persistent organic pollutants in this study. It affects several specific pathways (e.g., CYP450 metabolism, endocrine system) and causes morphological defects in developing zebrafish (e.g., pericardial edema; Hahn 2001; Jönsson et al. 2007).

Material and methods

Chemicals

Chemicals used for exposure were methylmercury (CAS 115-09-3; 60 µg/l), chlorpyrifos (CAS 2921-88-2; 7 mg/l in 0.01% ethanol), and Aroclor 1254 (CAS 11097-69-1, lot: LB 68958; 71.9 mg/l in 0.01% ethanol). All chemicals were purchased from Sigma-Aldrich, MO, USA.

Exposure

Wild-type zebrafish embryos (strains AB and ABO) were harvested, sorted for proper development, and exposed to three different chemicals and the controls at 28 °C from 24 to 48 hpf. Eggs were not dechorionated. Controls were done in embryo water (60 µg/ml Instant Ocean, Red Sea, Houston, TX, USA, pH 6.73, Ca 0.8 mg/l; K 0.6 mg/l; Mg 2 mg/l; Na 16 mg/l; S 2 mg/l; Westerfield 2000) separately for the exposure scenario to methylmercury and in 0.01% ethanol for the exposure scenario to chlorpyrifos and Aroclor 1254. To define the concentration, which was used for the microarray experiments, the embryos were transferred to control medium (ISO water) until 96 hpf. The microarray test concentration was then determined as the EC_{50} at 96 hpf. For the microarray experiments, the embryos were collected at 48 hpf (Yang et al. 2007). Only embryos that did not show any visual malformations were used for the microarray experiments. Each exposure and corresponding control was done at least three times individually and was subsequently processed independently in the microarrays. This approach allowed accounting for possible batch effects in single samples. For each sample, approx. 50 embryos were pooled. After exposure, the embryos were shock-frozen in liquid nitrogen and stored at −80 °C.

Microarray

For total RNA extraction, 1.5 ml Trizol Reagent (Life Technologies) was added and the embryos were homogenized using a disperser using RNeasy Mini Kit (Qiagen; see Yang et al. 2010). Subsequent steps were carried out according to the manufacturer's instructions. After phase separation, RNA precipitation and washing, the pellet was dissolved in 20 μL RNase-free water. The integrity of total RNA was checked on a denaturing agarose gel. The 28S ribosomal RNA (rRNA) and 18S rRNA of all samples appeared as two bands with an approximate ratio of 2:1. Concentrations and the 260/280 absorbance ratios were measured with a NanoDrop spectrometer (Thermo Scientific, Wilmington, DE, USA). Samples below a ratio of 1.6, hence contained protein impurities, were discarded.

The two-color microarray design was based on the zebrafish genome 4 × 44 k chip version 2 by Agilent (Agilent Technologies, USA). To avoid gene-specific dye effects, the experiment was replicated with reverse labeling (dye-swap) to balance the green and red dyes. The two microarrays with reverse-labeled probes were regarded as technical replicates. Chemically exposed and corresponding control embryos were compared and measured in triplicate repeats of the exposures. The assay was performed according to Agilent Low RNA Input Linear Amplification Kit Protocol (Agilent Technologies). In brief, 2 μg of total RNA from each sample was reverse-transcribed into complementary DNA (cDNA). Complementary DNA (cRNA) was transcribed from the cDNA and labeled with Cyanine3 (Cy3)-CTP and Cy5-CTP fluorescent dyes (Agilent Technologies). The cRNA samples were purified with the RNeasy Mini Kit and fragmented. The probes were put on the cover slips and chips, were placed in hybridization chambers, and incubated at 42 °C for 16–18 h, according to the manufacturer's protocol. For technical reasons, replicates for at least one exposure scenario (three biological replicates × two technical replicates) were handled in one run. Arrays were scanned using the Axon model 4000B dual-laser scanner and the corresponding GenePixPro 6.1 software (Axon, Union City, CA, USA). Both channels (532 nm for Cy3 and 635 nm Cy5) were scanned in parallel and stored as 16-bit TIFF files. The scans were performed with a resolution of 5 μm. Each array was scanned with an optimized signal amplification factor (voltage settings of the photomultiplier tubes). The channels for Cy3 and Cy5 were balanced in each scan for approximately the same intensity profile. The microarray data were submitted to Gene Expression Omnibus (GEO) with the accession number GSE88703 (Aroclor 1254), GSE88704 (chlorpyrifos), and GSE37970 (methylmercury).

Data analysis

The signal intensity information was extracted from the array images by the GenePix software according to the procedure provided by the manufacturer (Molecular Devices, CA, USA). After opening the TIFF image and loading the array list file, a grid with information to all spots was laid on the image data. The image information was extracted from every spot and transferred to a gpr-file with parameters, such as foreground and background pixels and Cy5 (532 nm) and Cy3 (635 nm) intensities. Background fluorescence occurs due to non-specific binding and should be corrected. The following processing of raw data, quality control, and analysis of variance was done according to the method described by Legradi (2011). In brief, raw data (i.e., fluorescence intensities of spots) were log transformed and normalized before statistical analysis. Differences in gene expression were represented as the differences between channels, $M = \log_2 (y_{red}) - \log_2 (y_{green})$, y = spot intensity. Systematic multiplicative error terms become additive and are automatically eliminated by subtracting the channel intensities. Spots with bad quality were removed from the dataset prior to further analysis. MA-plots (not shown) were used for quality control where M represents the log ratio of raw intensities ($\log_2 (y_{red}) - \log_2 (y_{green}) = \log_2 y_{green}/\log_2 y_{red}$) and A represents the average expression level of the spot ($\log_2 (y_{red} + y_{green})/2$). Log$_2$ fold-changes were calculated as mean of M values of both technical replicates (dye-swaps). The data were normalized by a chip wide analysis and a locally weighted regression smoother (LOESS). Gene-specific standard error and global standard error among all genes were weighted to account for the small sample size.

After aggregation of the normalized log$_2$ fold-changes from all three treatments, statistical quality criteria were applied. Pre-selection of fold-changes was applied to ensure that at least two fold-change values for each treatment were included in the analysis. If there was a missing value for one treatment, the group median was imputed. Only genes with a mean absolute fold-change of at least 1 were selected for further analysis. Genes were grouped by treatments, with each group containing all genes with a mean absolute fold-change for the group treatment of at least 1.

The normalized log$_2$ fold-change datasets were subjected to ANOVA to detect significantly differently expressed genes after Levene's test had been performed to test for equal variances between the classes. A linear model was fitted to the data to check whether gene expression after exposure was actually significantly different from the control (Smyth 2004). Genes that passed all three statistical criteria (fold-change, ANOVA, linear model) were considered discriminative and used in pathway network analysis. An overview of the statistical analysis is given in Fig. 1. All analyses were performed using routines from the R statistical package (version 3.1.2).

A volcano plot (Li 2012) was used to depict (log$_2$) fold-changes against ANOVA log$_{10}$ p values. Volcano plots provide the possibility to combine fold-changes and ANOVA significance results. The mean fold-change was calculated for each
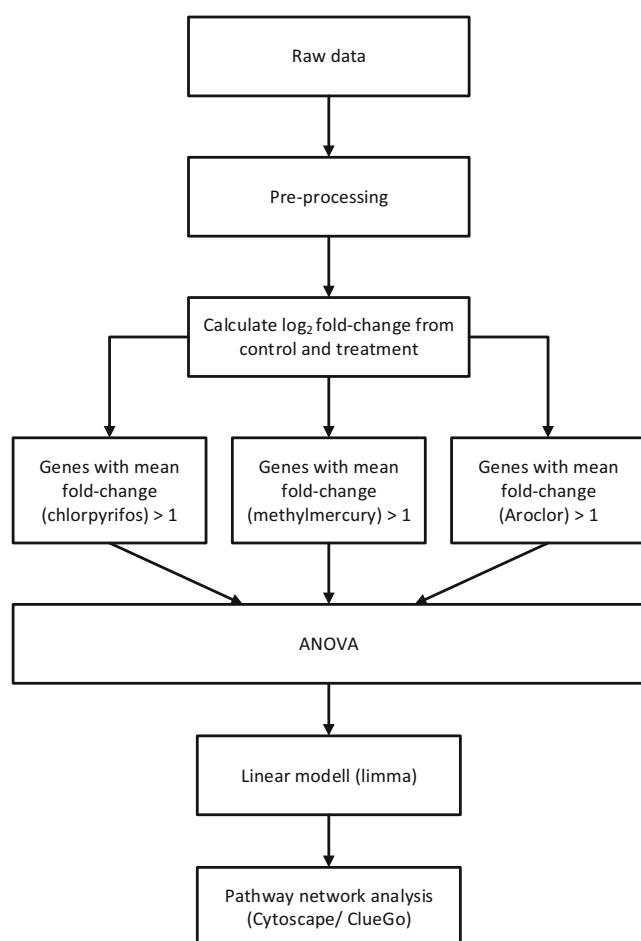
Fig. 1 Overview of the statistical analysis

gene and for all three treatments separately. This way, each gene provided three mean fold-changes. This enabled the examination of genes based on their variance and overall change in expression. In the volcano plot, each x value corresponded to the highest mean fold-change of a treatment group. Data points were colored according to the treatment group of which the corresponding genes were also significant according to linear regression. Non-discriminative (i.e., genes not taken forward in the analysis) genes were colored gray. Lines indicating a significance level of $\alpha = 0.05$ (horizontal) and fold-change thresholds of 1 and −1 (vertical) were added to the plot. These lines divide the genes of the volcano plot into four groups A, B, C, and D. Genes with a high fold-change and low p values in the volcano plot were considered most relevant (group A). Genes with a fold-change below a certain threshold were neglected even despite significant p values (group B) because in this case, the expression change is considered too small to have a biological impact (McCarthy and Smyth 2009). In addition, genes with an insignificant p value but large fold-changes were rejected, as these may have been influenced by high variance in the data (group D; Dalman et al. 2012; Xiao et al. 2014). The volcano plot was created using the R-package ggplot2.

Discriminative genes of all treatments were clustered hierarchically based on Euclidean distance and Ward's clustering (using the `heatmap.2` function from the R-package `gplots`) to create a color-scaled heatmap (Eisen et al. 1998; Murtagh and Legendre 2014). Clustering distance and algorithm are both proven to show good results for microarray data (Freyhult et al. 2010; Giancarlo et al. 2010). The heatmap visualized the relative expression and grouping of the discriminative genes across the different chemicals treatments and replicate arrays.

Pathway network analysis was performed using the discriminative genes, which were selected by the statistical criteria, to identify enriched functional ontology terms using Cytoscape plugin ClueGO 2.1.7 (Bindea et al. 2009). Gene ontology (GO) databases for biological processes, molecular functions, immune system processes, and cellular components were used for gene annotation (databases from October 05, 2015). GO tree interval was set to range from 3 to 8, the minimum number of genes per cluster was 2. Only significantly enriched terms were selected using right-sided hypergeometric tests with Benjamini-Hochberg correction ($p < 0.05$). The resulting network was drawn with a kappa score (minimum connectivity of the network) of 0.4 U. The analysis was carried out independently for each treatment, with up- and downregulated genes in separate clusters. To distinguish between up- and downregulated gene clusters within the terms, nodes were colored blue for up- and red for downregulation. Nodes with both up- and downregulated genes were colored gray. Node size was determined by the significance of enrichment, while edge width refers to kappa score of the connection. The same analysis was also done using the Kyoto Encyclopedia of Genes and Genomes (KEGG) pathway database. For better visibility, labels were edited using Inkscape 0.91.

Results

Differentially expressed genes

From initially over 14,000 genes, 4298 passed the statistical quality criteria. Only genes showing a mean $\log_2$ fold-change of at least +1 respectively −1 for at least one treatment were used in ANOVA. These genes were divided into three groups according to the treatment that inflicted the highest absolute mean fold-change. Results of Levene's test indicated that only 128 genes showed unequal variance ($p < 0.05$). This corresponded to less than 5% of all genes, and thus, we assumed equal variance. Genes for which the result of the ANOVA indicated a significant difference in expression for one of the three treatments were considered discriminative genes. This was done to separate them from genes involved in general stress responses, which tend to show differential

regulation in any chemical treatment. Such non-discriminative genes were excluded from the following analysis.

The remaining genes were tested for significantly different expression (according to linear regression, $\alpha < 0.05$) from the control expression values for each of the three chemical treatments separately. After the three filtering steps, namely fold-change cutoff, ANOVA, and linear regression, the remaining 312 genes were used for further analysis.

Overall, more genes were found significantly downregulated than upregulated (185 down, 127 up). Most genes were altered in their expression by methylmercury (148 genes, 47.4% of all genes); fewer genes were significantly influenced by Aroclor 1254 (122 genes, 39.1%) and the least by chlorpyrifos (42 genes, 13.5%). For methylmercury, 64% of the significantly regulated genes were downregulated; for Aroclor 1254, it was 54% and for chlorpyrifos 64%. The genes *matrix metalloproteinase 9* (*mmp9*) and *selenoprotein W, 1* (*sepw1*) showed the highest respectively lowest fold-changes of all genes (*mmp9* = 11.4-fold; *sepw1* = −5.8-fold), both in response to methylmercury (Table 1). Another matrix metalloproteinase (*mmp13a*; 8.1-fold) alongside *jun B proto-oncogene* (*junb;* 5.8-fold) and *jun B proto-oncogene, like* (*junbl*; 4.7-fold) were also significantly upregulated following methylmercury exposure. For exposure following chlorpyrifos, up- or downregulation of genes was overall not as strong as following the other two contaminants. *Annexin A1b* (*anxa1b*; 3.9-fold) and *cytokine inducible SH2-containing protein* (*cish*; 2.69-fold) were the most highly and significantly expressed genes. Among the significant genes following exposure to Aroclor 1254, *cytochrome P450, family 1, subfamily A* (*cyp1a*) stood out as being the strongest upregulated gene by far (7.9-fold).

Volcano plot and heatmap

A volcano plot was drawn to visualize the main characteristics of the transcriptome response (Fig. 2) in terms of response strength and regulation. Genes located in the upper right and left quarter of the plot (Fig. 2, group A) have both a large mean fold-change and a small p value. Genes clustered at the bottom center of the plot (group C) have insignificant p values and small mean fold-changes. Genes in group B have also small mean fold-changes but significant p values while genes in group D have insignificant p values and large mean fold-changes.

The heatmap (Fig. 3) was used to translate fold-changes into a color code to facilitate the detection of gene expression patterns and contaminant class-specific transcriptome signatures. Gene-wise hierarchical clustering formed three distinct clusters, corresponding to the three treatments. Within these clusters, patterns of up- and downregulated genes can be found unique to each

Table 1 Most highly expressed genes for each of the three treatments

Gene symbol	Gene name	Mean fold-change		
		chlor	mehg	pcb
Chlorpyrifos				
*anxa1b**	Annexin A1b	3.88	−0.19	−0.31
gc	Vitamin D binding protein	−2.84	−0.62	−0.53
*cish**	Cytokine inducible SH2-containing protein	2.69	−0.13	−0.71
sec61g	Sec61 gamma subunit	1.98	0.92	0.66
*ndufa2**	NADH dehydrogenase (ubiquinone) 1 alpha subcomplex, 2	1.95	−0.05	0.18
Methylmercury				
*mmp9**	Matrix metalloproteinase 9	0.99	11.44	1.2
*socs3a**	Suppressor of cytokine signaling 3a	0.42	8.1	0.3
*mmp13a**	Matrix metalloproteinase 13	0.33	8.08	2.12
*zgc:103438**	si:dkey-228a15.1	0.18	7.2	0.4
*socs3b**	Suppressor of cytokine signaling 3b	0.67	6.67	0.93
Aroclor 1254				
*cyp1a**	Cytochrome P450, family 1, subfamily A	3.57	0.43	7.9
*fkbp5**	FK506 binding protein 5	−2.46	1.14	−3.82
*itgb1b.2**	Integrin, beta 1b.2	−0.50	−1.1	−3.22
*tnni2b.1**	Troponin I, skeletal, fast 2b.1	−1.01	−0.15	2.96
*mat1a**	Methionine adenosyltransferase I, alpha	−0.65	−0.5	−2.89

Fold-changes of the genes for each treatment are shown. List includes five genes with highest absolute fold-changes for each treatment (mehg = methylmercury, chlor = chlorpyrifos, pcb = Aroclor 1254). Genes marked with an asterisk are significant according to ANOVA.
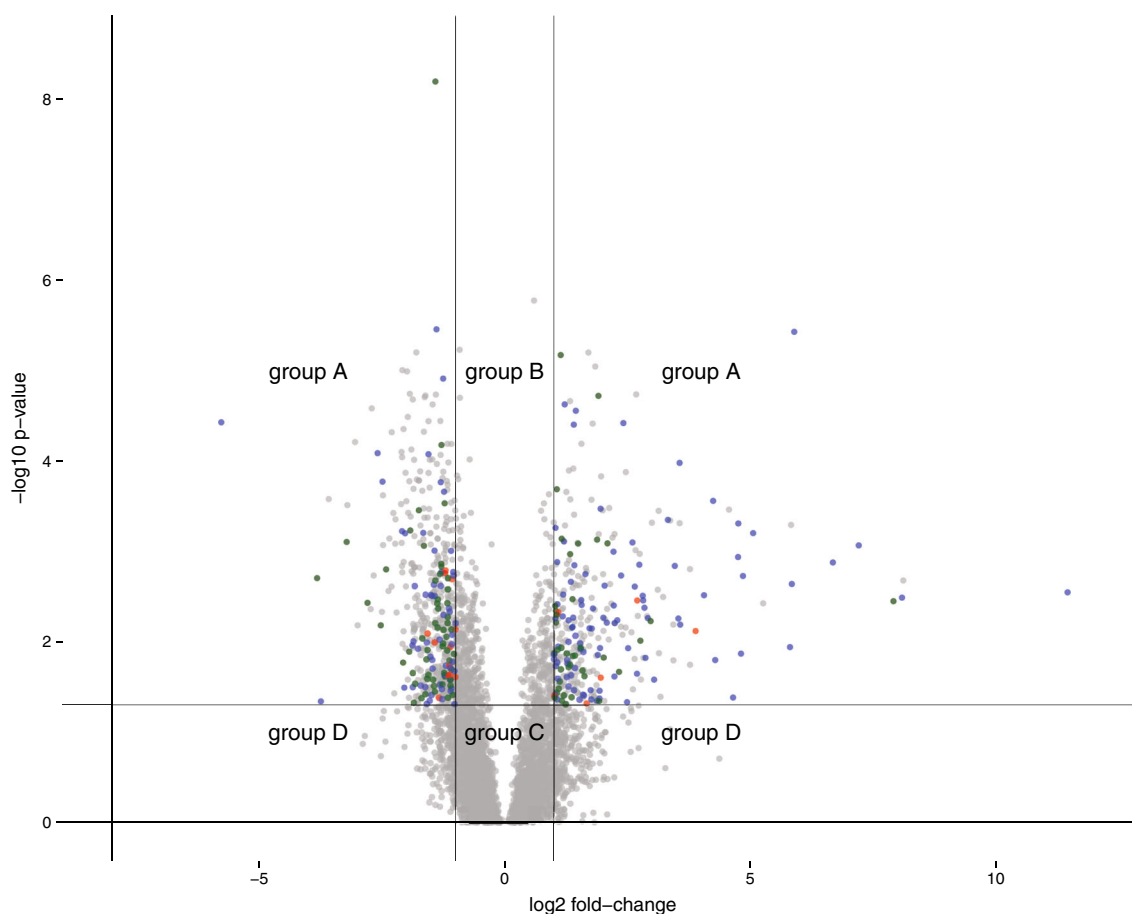
Fig. 2 Volcano plot of the microarray data from all three treatments. The horizontal *x*-axis depicts the highest group mean fold-change; the vertical *y*-axis shows the statistical ANOVA significance. Larger values on the *vertical axis* represent larger statistical significance. Points were colored according to the (treatment) group. *Blue* indicates genes that showed the highest mean fold-change after exposure to methylmercury, *green* to Aroclor 1254, and *red* to chlorpyrifos. Non-discriminative genes were colored *gray*. The *horizontal line* corresponds to the ANOVA cutoff *p* value of 5%; the *vertical lines* correspond to a fold-change of 1 and −1. The genes were divided into four groups *A*, *B*, *C*, and *D*, according to the *horizontal and vertical lines*. Volcano plot was drawn using the R-package `ggplot2` (R-version 3.1.2)

treatment and suitable to distinguish them. Methylmercury induced a more distinct expression profile, which is clearly separated from chlorpyrifos and Aroclor 1254. Gene expression patterns of chlorpyrifos and Aroclor 1254 are partially similar but at least one pattern can be used to distinguish each treatment from the other. Additionally, there are no gene patterns similar in reaction to all treatments, indicating the initially intended exclusion of general stress-related genes.

Pathway network analysis

Significantly regulated genes were subjected to a pathway network analysis to identify functional enrichment. For methylmercury (Fig. 4), more red than blue nodes indicated a stronger over-representation of downregulated than upregulated genes among the significant functional terms. Downregulated GO-groups (groups of two or more connected terms) were appendage morphogenesis, chloride channel activity, fructose 2,6-bisphosphate metabolic process, nucleophagy, protein peptidyl-prolyl

isomerization, and regulation of target of rapamycin (TOR) signaling. The only significant GO-group composed of mostly upregulated genes was small molecule catabolic process. For lists of all over-represented GO-groups and contained functional terms, see Additional file 1.

The exposure to Aroclor 1254 (Fig. 5) resulted in downregulated genes which were significantly over-represented in the GO-groups histone acetyltransferase complex, intracellular protein transmembrane transport, protein folding, and protein import into mitochondrial matrix. Upregulated by Aroclor 1254 were autophagosome and response to hypoxia. Many of the Aroclor 1254 exposure-enriched terms were mitochondrion-related and downregulated (mitochondrial membrane organization, mitochondrial transmembrane transport, protein targeting to mitochondrion, protein localization to mitochondrion, and establishment of protein localization to mitochondrion).

Results of the pathway network analysis for chlorpyrifos (Fig. 6) showed fewer (8 terms) over-represented terms than the other two treatments (methylmercury, 60 terms; Aroclor

Fig. 3 Heatmap-clustering (Euclidean distance, Ward's clustering) of all discriminative genes. Upregulation is depicted in *blue*, downregulation in *red* (according to fold-change; color code in the *top right*). Genes are clustered on the *left*; replicated arrays for the three treatments on *top* (*chlor* chlorpyrifos, *mehg* methylmercury, *pcb* Aroclor 1254). The heatmap was calculated using the `heatmap.2` function from the R-Package `gplots` (R-version 3.1.2)
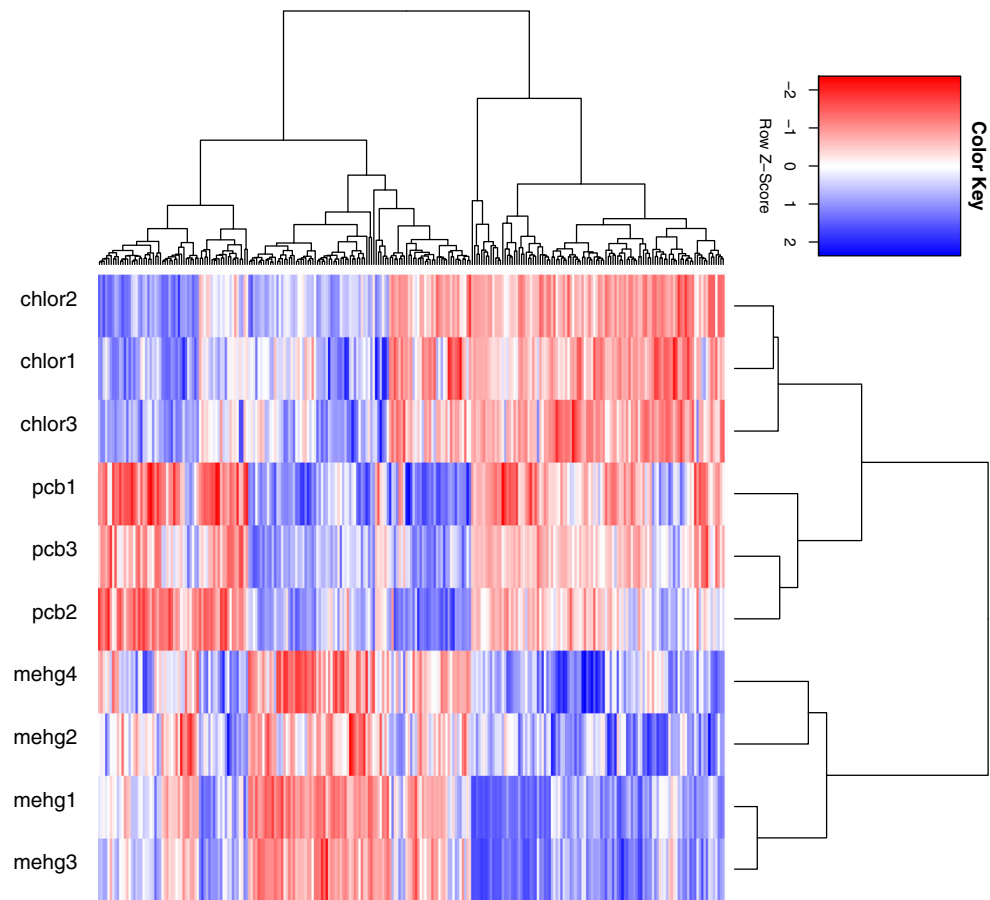
1254, 46 terms). These terms were significantly over-represented ($\alpha < 0.05$) by downregulated genes. They belonged to the GO group coagulation, DNA packaging complex, and anion channel activity.

Alternatively, KEGG pathway analysis detected substantially less significantly enriched nodes than GO. The exposure to methylmercury significantly changed the expression of genes in the KEGG pathways peroxisome proliferator-activated receptors (PPAR) signaling pathway and fatty acid degradation (both downregulated). For Aroclor 1254 peroxisome (downregulated), retinol metabolism and nicotinate and nicotinamide metabolism (upregulated) were significantly enriched KEGG pathways. No KEGG pathways were significantly changed following exposure to chlorpyrifos.

Discussion

In the present study, we analyzed the microarray experiments first separately for each of the three chemicals and calculate gene fold-changes using corresponding controls (baseline) for each treatment. ANOVA was then performed on the fold-change data of all three treatments instead of pairwise *t* statistics to prevent error accumulation due to multiple testing

(Churchill 2004). This way, it was possible to detect transcriptome signatures that were contaminant class-specific.

Volcano plot

By depicting the results of all three contaminants in the volcano plot, the highest fold-changes and thus the strength of the reaction of the whole zebrafish genome could be assessed in parallel. According to the number of colored points in group A, the strongest gene response was induced by the exposure to methylmercury (blue points, Fig. 2) while chlorpyrifos provoked the weakest response (red points).

The densest accumulation of points occurred, as expected, in group C. However, many genes (compared to the number of genes of group A) fell into group D or B. These genes showed either large fold-changes with insignificant *p* values (D) or small fold-changes with significant *p* values (B). These results can be explained by the fact that we performed an ANOVA, which allowed us to compare the results from all three treatments simultaneously. All three contaminants influenced genes in group D, explaining the lack of significant difference despite the comparatively large fold-change values in comparison to the treatment corresponding controls. The fold-changes did not result in significant ANOVA *p* values since
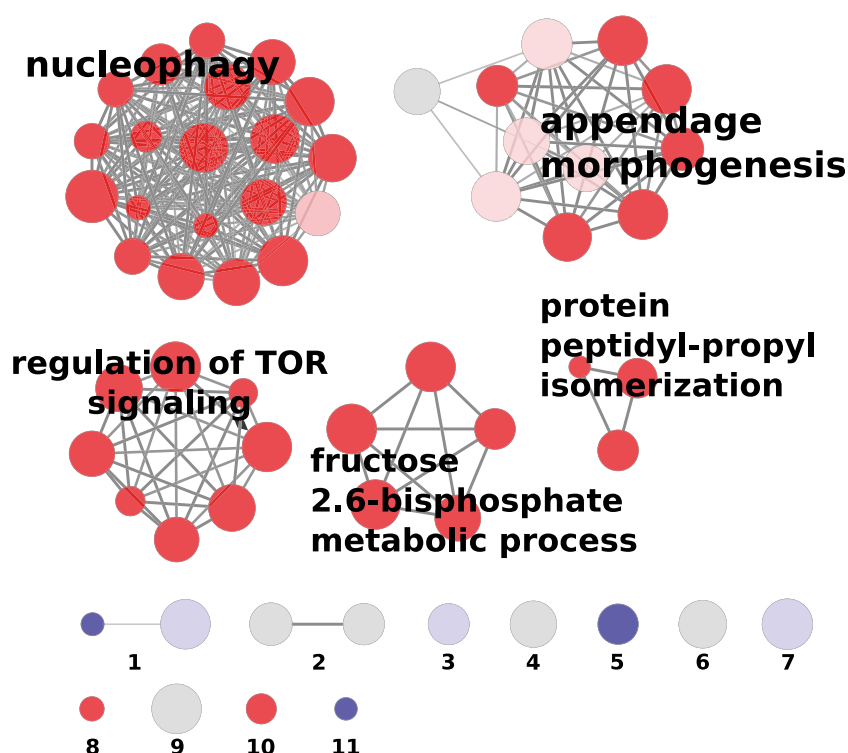
Fig. 4 Pathway network of significantly over-represented GO-terms following treatment of methylmercury. *Nodes* represent significantly differentially expressed genes that are similar in function; *edges* represent pairwise interactions. *Red nodes* include downregulated genes; *blue nodes* depict upregulated genes. *Gray nodes* were not especially over-represented. Functional groups with less than three nodes are labeled with a number: *1* = small molecule catabolic process, *2* = chloride channel cell chemotaxis, *3* = cell chemotaxis, *4* = transition metal ion homeostasis, *5* = positive regulation of response to external stimulus, *6* = retinal ganglion cell axon guidance, *7* = response to toxic substance, *8* = sodium ion transport, *9* = cellular aldehyde metabolic process, *10* = dicarboxylic acid transmembrane transporter activity; *11* = metalloendopeptidase activity. A list of all over-represented terms, as well as the same figure with all labeled terms, is provided in Additional file 1

these genes were equally differentially expressed in all three treatments. This most likely applies to genes involved in more general processes such as detoxification. The challenge to distinguish these genes from the ones involved in more specific response pathways, common to gene expression analyses (Kosmehl et al. 2012), was met by our analysis. It allowed us to filter out genes, which are unsuitable as discriminators for specific contaminant classes.

If a gene hardly responded to one of the treatments but strongly to both other treatments, this gene was classified into group B as being significantly differently exposed. Using a post-hoc test here would lead to a wrong conclusion, indicating that the treatment, to which the gene had not responded to, was the most relevant. Using a fold-change cutoff and a linear model, we considered this negative indication and avoided this potential issue.

According to the linear model, some genes were not identified as discriminative despite significant difference according to ANOVA and an above threshold fold-change for one of the treatments. These genes occurred as gray points in group A. Genes of group B which showed a weak but significant response to one treatment but a small gene expression variance in the other two treatments were considered to be of

limited importance for a pathway network analysis. Nevertheless, despite the small variance (resp. sensitivity) in response to a treatment, they could still be discriminative for this contaminant class. Pavlidis (2003) showed that small fold-changes can be important in a certain biological context. For example, when investigating gene expression in the nervous system, small changes are often more relevant than in other parts of the organism. Therefore, it is not recommended to use a common fold-change threshold for different experiments. The volcano plot can help identifying patterns or groups and picking relevant genes. Therefore, it can be a good quality control measure to the results of the statistical tests.

Pathway network analysis

All over-represented pathways (terms) for chlorpyrifos contained downregulated genes. The number of genes, which were differentially expressed, was significantly lower than for the other two treatments. Chlorpyrifos is known to inhibit acetylcholinesterase (ache), which is important in neurotransmission as it hydrolyzes acetylcholine to choline and acetate thereby terminating synaptic transmission (Straus and Chambers 1995; Kwong 2002). It was already shown that
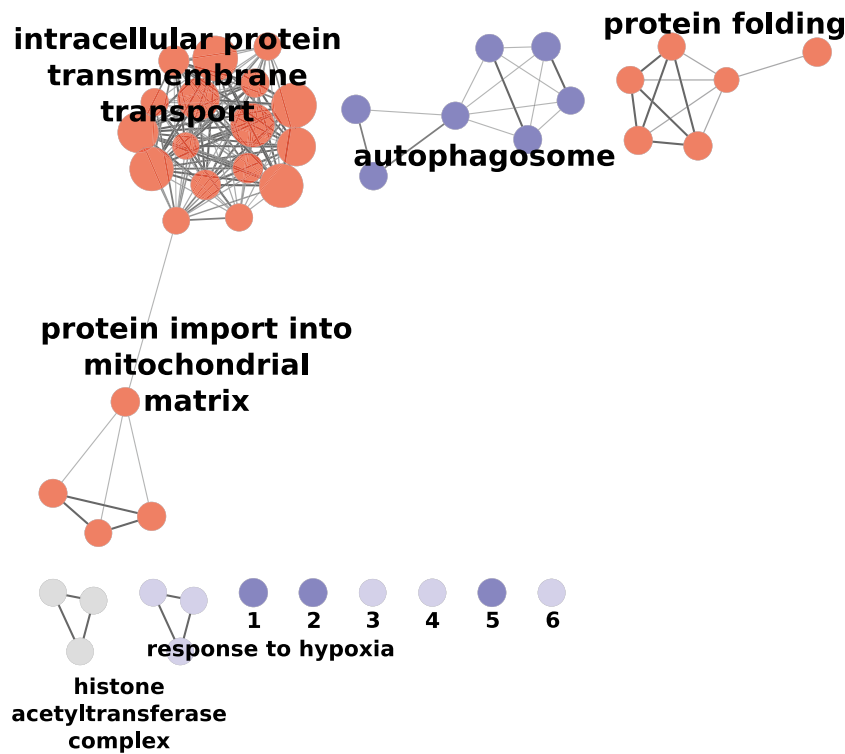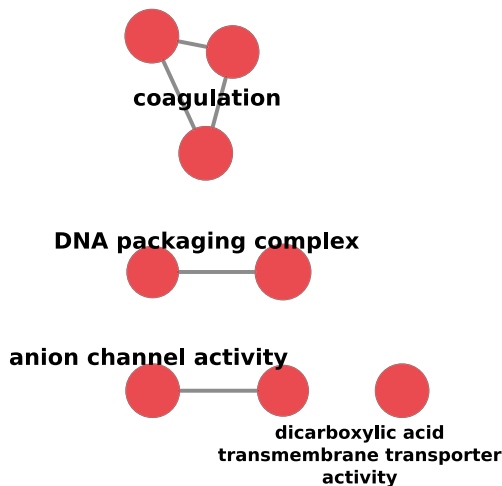
Fig. 5 Pathway network of significantly over-represented GO-terms following treatment of Aroclor 1254. *Nodes* represent significantly differentially expressed genes that are similar in function; *edges* represent pairwise interactions. *Red nodes* include downregulated genes; *blue nodes* depict upregulated genes. *Gray nodes* were not especially over-represented. Functional groups with less than three nodes are labeled with a number: *1* = integral component of endoplasmic reticulum membrane, *2* = negative regulation of cell cycle process, *3* = integrin-mediated signaling pathway, *4* = mitochondrial outer membrane, *5* = metalloendopeptidase activity, *6* = transition metal ion transport. A list of all over-represented terms, as well as the same figure with all labeled terms, is provided in Additional file 1

acetylcholinesterase is critical for the neuronal development of zebrafish (Behra et al. 2002). In contrast to our expectation,

Fig. 6 Pathway network of significantly over-represented GO-terms following treatment of chlorpyrifos. Nodes represent significantly differentially expressed genes that are similar in function; edges represent pairwise interactions. *Red nodes* depict downregulated genes. No terms with upregulated genes were significantly enriched. A list of all over-represented terms, as well as the same figure with all labeled terms, is provided in Additional file 1

a significant upregulation of *ache* to compensate the inhibition of the enzyme by chlorpyrifos was not detected. This may be attributed to low uptake and reduced metabolism of chlorpyrifos by the embryos as proposed by Legradi (2011). Yang et al. (2011) could not detect an effect on ache activity after chlorpyrifos exposure from 24 to 48 hpf. However, they found a change in ache activity after exposure to chlorpyrifos-oxon, a metabolite of chlorpyrifos. On protein level, also no effects on ache after chlorpyrifos exposure during the first 24 h of development were seen (Liu et al. 2015). When exposed from 6 hpf to 5 dpf, significant ache activation can be observed (Yen et al. 2011) indicating that chlorpyrifos is only inhibiting ache activity after 48 hpf. This might have to do with the minimal metabolic capability of the embryo prior 48 hpf. Chlorpyrifos needs to be bioactivated via transformation into its oxon form. An explanation for the overall low number of significant genes and pathways might be that the exposure time was too short, and chlorpyrifos was not present as activated chlorpyrifos-oxon (Yang et al. 2011).

In a recent study, Lewis et al. (2014) showed that *cish*, which can be found in the group of the significantly regulated genes for chlorpyrifos (Table 1), has a key function in the embryonic hematopoiesis. In particular, they observed enhanced embryogenic erythropoiesis, myelopoiesis, and lymphopoeisis in morpholinos

targeting *cish*. Hematotoxicity is one of many known toxic effects of chlorpyrifos (Uzun and Kalender 2013). However, besides the alteration of the production of reactive oxygen species (ROS), little is known about the underlying mechanism of this effect (Demir et al. 2011). The downregulation of *cish* could be a possible mechanism of chlorpyrifos-induced hematotoxicity. One explanation for the overall low number of significantly regulated genes and pathways might be due to the exposure during the first 2 days of embryogenesis, in which embryos are still protected by the chorion and, in addition, might lack the capacity to metabolize chlorpyrifos to the more toxic chlorpyrifos-oxon as suggested by Yang et al. (2011).

As for methylmercury, several significantly enriched terms were related to fin morphogenesis including embryonic pectoral fin morphogenesis (downregulated), embryonic appendage morphogenesis (downregulated), and fin regeneration (upregulated; Fig. 4) suggesting an effect of methylmercury on the fin development of *D. rerio*. Yang et al. (2007, 2010) proved in two studies that methylmercury causes the suppression of the tail primordium of zebrafish embryos. The authors conducted microarray experiments with multiple contaminants in 2007 and further characterized the mechanism of action of methylmercury morphologically in addition to using in situ hybridization in 2010. They used concentrations of methylmercury and exposure times similar to this study. The developmental toxicity was linked to tissue damage and disturbance of the cellular homeostasis of the fin fold. Yang et al. (2010) found that instead of forming a clear, fan-shaped find fold, the membrane surrounding the tail was smaller and less structured. These results were in line with other studies describing appendage malformations following methylmercury exposure (Samson and Shenker 2000; Keiter et al. 2013).

Following exposure to methylmercury, we expected metalloproteases to be upregulated. Yang et al. (2010) found a strong upregulation of two matrix metalloproteases (*mmp9* and *mmp13*) in combination with the modified development of the fin fold and the tail fin primordium, corroborating the hypothesis of an impairment of fin development by methylmercury. The current study confirmed the results on *mmp9* and *mmp13* which were 11.4- and 8.1-fold upregulated after exposure to methylmercury (Table 1). Both genes were among the genes showing the strongest change in expression of all tested genes. Following exposure to chlorpyrifos or Aroclor 1254, the two genes did not show comparable induction levels (chlorpyrifos: *mmp9*: 1.0-fold, *mmp13*: 0.3-fold; Aroclor 1254: *mmp9*: 1.2-fold, *mmp13*: 2.1-fold). These results are in accordance with both studies of Yang et al. (2007, 2010). In 2007, the authors found *mmp9* to be upregulated 6.7-fold and *mmp13* 5.9-fold in their microarray analysis. By using whole-mount in situ hybridization, they were able to link this upregulation to the effects on the tail fin primordium in their later study (Yang et al. 2010). Their results indicated that misregulation of *mmp9* and *mmp13* leads to tissue damage in the fin fold as metalloproteases could play a role in tissue

regeneration (Bai et al. 2005). In this study, we suggest that within the range of the chemicals, tested *mmp9* and *mmp13* serve as useful discriminative genes to identify the effect of methylmercury.

Moreover, *junb* and *junb-like* (*junbl*) were upregulated following methylmercury exposure: *junb* 5.8-fold and *junbl* 4.7-fold. Ho et al. (2013) found comparable upregulation of *junb* and *junbl* following methylmercury (*junb* 7.4-fold and *junbl* 4.8-fold). These genes are known to play a role in zebrafish tissue regeneration and especially in regenerating fin and fin fold (Ishida et al. 2010). This could be an indication of a compensatory effect to the methylmercury-induced developmental toxicity, which inflicts tissue damage in the fin fold.

Exposure to Aroclor 1254 resulted in changes of mitochondria-related pathways at multiple functional levels including mitochondria structure and function, protein folding and transport, reduced oxygen level, and autophagosomes among others (Fig. 5). These results are in line with several other studies showing disruptive effects of PCBs on mitochondrial oxidative phosphorylation (Nishihara and Utsumi 1987), decreased respiratory control (Nishihara 1985), electron transfer (Nishihara et al. 1986), and ROS generation (Fujita et al. 2006) for rat and marine fish species (Schlezinger et al. 2006). Aroclor 1254 is known to impair oxidative phosphorylation, which could explain the strong effect on mitochondrial and oxygen depletion related pathways. Mitochondria have shown to be the earliest and most important cell targets in Aroclor-mediated toxicity (Aly et al. 2009; Aly and Domènech 2009).

Aroclor 1254 generally is considered as a strong inducer of *cyp1a* not only in fish (Shelton et al. 1986; Chaty et al. 2004) but also in other vertebrates for instance rats or humans (Silkworth et al. 2005; Borlak and Jenke 2008). In accordance with these studies, *cyp1a* showed the highest absolute mean fold-change of all genes that reacted significantly to Aroclor 1254 in this study (7.9-fold; Table 1). According to Schlezinger et al. (2006), PCB can cause oxidative stress by uncoupling the catalytic cycle of cyp1a, thereby enhancing ROS production. This might be an important mechanism of Aroclor 1254 toxicity in the fish embryos. Results from Liu et al. (2014) suggest that oxidative stress represents a major factor in the induction of various developmental alterations in early life stages of zebrafish exposed to PCB. Moreover, our results show that transcripts of genes belonging to pathways related to cellular oxygen level and response to hypoxia (both GO) and peroxisome (KEGG) were also enriched following exposure to Aroclor 1254 further supporting our findings suggesting an oxidative stress response. Additionally, a few studies suggested that *cyp1a* and the aryl hydrocarbon receptor (AhR) pathway are involved in more specific toxicity, in particular abnormal development of zebrafish, e.g., embryonic craniofacial and cardiovascular malformations, circulatory failure, edemas, and hemorrhages (Henry et al. 1997;

Handley-Goldstone et al. 2005; Carney et al. 2006; Jönsson et al. 2007). Several knockdown studies have shown crosstalk between the AhR and other signaling pathways underlining the importance of *cyp1a* for specific toxic endpoints. For example, Jönsson et al. (2012) demonstrated that the effects of PCB126 on inflation of the swim bladder are depending on the AhR and that treatment with a morpholino to knock down AhR rescued the effect of PCB126 on the developing swim bladder in zebrafish. Another study showed that exposure to 2,3,7,8-tetrachlorodibenzo-*p*-dioxin (TCDD) causes AhR dependent misregulation of Wnt/β-catenin target genes thereby altering the differentiation and/or the proliferative status of liver progenitor cells (Prochazkova et al. 2011). Further studies are required to underpin this connection.

Alongside the already mentioned alterations of the peroxisome pathway, retinol metabolism was one of the significantly over-expressed KEGG pathways, indicating an effect of the AhR pathway on the photoreceptor development. The aryl hydrocarbon receptor repressor (AHRR) is a transcriptional repressor of the AhR and is regulated by an AhR-dependent mechanism. Zebrafish possess two AHRR paralogs: AHRRa regulates constitutive AHR signaling during development, whereas AHRRb regulates PAH-induced gene expression. Aluru et al. (2014) conducted microarray-based whole-genome mRNA analyses on zebrafish embryos with morpholino knocked down zfAhRRa or zfAhRRb. Among the downregulated genes by zfAhRRa knockdown, several were related to photoreceptor function of the eye (opsins, phosphodiesterases, phosducin, arrestins, and retinol binding protein), suggesting that AHRRa affects photoreceptor development, which is in line with our KEGG pathway analysis results.

Salvi and Toninello (2001) found that Aroclor 1254 can influence the mitochondrial permeability transition (MPT). A sudden increase in the permeability of the mitochondrial inner membrane leads to a colloid osmotic swelling of the organelle. This process takes place when large amounts of Ca^{2+} are accumulated in the matrix space of the mitochondrion. In this study, several enriched functional terms following Aroclor 1254 exposure can be linked to MTP, including mitochondrial membrane organization, mitochondrial transport, protein import into mitochondrial matrix, and mitochondrial outer membrane as well as necrosis and apoptosis (Bradham et al. 1998; Fujita et al. 2006). The induction of apoptosis is an important process to eliminate tumor cells, and the suggested MPT-inhibiting effect of Aroclor 1254 might provide a possible explanation for the carcinogenic effect of PCBs (Salvi and Toninello 2001). Aly and Domènech (2009) investigated the effects of Aroclor 1254 on hepatocyte mitochondria of rats and found that Aroclor 1254 inhibited β-oxidation of fatty acid and mitochondrial respiratory chain complexes. These findings were in coherence with our experiments on Aroclor 1254 in which terms were enriched for mitochondrial membrane function and composition (downregulated). The goal of our analysis was to exclude general effects that are not specific to a certain treatment. Oxidative stress is considered to be a more general process. However, Yang et al. (2007) showed that there is no general, contaminant unspecific response to oxidative stress in zebrafish. Instead, genes induced by oxidative stress can differ between treatments suggesting contaminant-specific effects. This is in line with our results as we detected very specific genes and pathways related to oxidative stress. Additionally, our analysis included only genes reacting specific to one of the treatments making it more likely that the responses are substance class-specific. Genes related to oxidative stress (e.g., catalase, glutathione peroxidase) also showed a change in expression following exposure to methylmercury (data not shown), which is considered to be a major enabler of oxidative stress in zebrafish (Richter et al. 2011; Cambier et al. 2012). These genes were excluded (by our algorithm) from pathway network analysis because their reaction was not specific to one of the treatments.

Although the results were overall promising, there were some limitations of the study, which have to be mentioned. We used only a single exposure concentration and time for each treatment. At different stages of the zebrafish development or after exposure to various test concentrations, the selected genes might be expressed differently. It is possible that internal concentrations have not reached a state of equilibrium at 48 hpf due to different toxicokinetics possibly affecting gene responses.

Consequently, further studies are required to confirm the specific transcriptome signatures of methylmercury, chlorpyrifos, and Aroclor 1254. Moreover, real-time polymerase chain reaction could be used to ensure specificity and robustness of the results. We selected three chemicals that represent ecotoxicologically relevant substance classes to find substance class-specific effects. For methylmercury, we were able to detect very specific genes and pathways which could be linked to certain mechanism-specific effects and were in line with our hypothesis. For Aroclor and chlorpyrifos, however, fewer genes were found overall and the detected effects were both specific and general. In order to fully exploit the potential of our approach, an extension of the analysis using more substance classes is needed. This would not only reveal specific genes and pathways for a greater number of contaminant classes but would also improve the performance and results for each substance class by ultimately excluding more and more general genes and pathways.

Conclusions

In the present study, we demonstrated that our approach of transcriptome analysis can be very successful in defining discriminative genes for different classes of contaminants. Limiting the further analysis of the data to these discriminative

genes and finding transcriptome signatures increases the chance of detecting genes that play important roles in contaminant class-specific regulatory pathways (as shown for fin morphogenesis in response to exposure to methylmercury). The selected genes and transcriptome signatures can be relevant in the proposed concept of a barcode-like identification of toxic substances in biological samples (Lettieri 2006; Yang et al. 2007) or as a part of an adverse outcome pathway (AOP) if combined with information from different levels of biological organization (Van Aggelen et al. 2010; Villeneuve et al. 2014a, b). Thereby, given further studies with other contaminant classes and perhaps even mixtures for verification, our results may be implemented in environmental monitoring or risk assessment.

In conclusion, contaminant class-specific discriminative genes and transcriptome signatures could effectively be extracted from microarray data of zebrafish embryos. However, further investigations with more substance classes and the development of robust statistical approaches are required to verify and enhance our findings.

Compliance with ethical standards

Conflict of interest   The authors declare that they have no conflict of interest.

References

Aluru N, Jenny MJ, Hahn ME (2014) Knockdown of a zebrafish aryl hydrocarbon receptor repressor (AHRRa) affects expression of genes related to photoreceptor development and hematopoiesis. Toxicol Sci 139:381–395. doi:10.1093/toxsci/kfu052

Aly HAA, Domènech Ò (2009) Aroclor 1254 induced cytotoxicity and mitochondrial dysfunction in isolated rat hepatocytes. Toxicology 262:175–183. doi:10.1016/j.tox.2009.05.018

Aly HAA, Domènech Ò, Abdel-Naim AB (2009) Aroclor 1254 impairs spermatogenesis and induces oxidative stress in rat testicular mitochondria. Food Chem Toxicol 47:1733–1738. doi:10.1016/j.fct.2009.03.019

Bai S, Thummel R, Godwin AR et al (2005) Matrix metalloproteinase expression and function during fin regeneration in zebrafish: analysis of MT1-MMP, MMP2 and TIMP2. Matrix Biol 24:247–260. doi:10.1016/j.matbio.2005.03.007

Bartosiewicz M, Penn S, Buckpitt A (2001) Applications of gene arrays in environmental toxicology: fingerprints of gene regulation associated with cadmium chloride, benzo(a)pyrene, and trichloroethylene. Environ Health Perspect 109:71–74. doi:10.1289/ehp.0110971

Behra M, Cousin X, Bertrand C et al (2002) Acetylcholinesterase is required for neuronal and muscular development in the zebrafish embryo. Nat Neurosci 5:111–118. doi:10.1038/nn788

Bindea G, Mlecnik B, Hackl H et al (2009) ClueGO: a cytoscape plug-in to decipher functionally grouped gene ontology and pathway annotation networks. Bioinformatics (Oxford, England) 25:1091–1093. doi:10.1093/bioinformatics/btp101

Borlak J, Jenke HS (2008) Cross-talk between aryl hydrocarbon receptor and mitogen-activated protein kinase signaling pathway in liver cancer through c-raf transcriptional regulation. Molecular cancer research : MCR 6:1326–1336. doi:10.1158/1541-7786.MCR-08-0042

Bradham CA, Qian T, Streetz K et al (1998) The mitochondrial permeability transition is required for tumor necrosis factor alpha-mediated apoptosis and cytochrome c release. Mol Cell Biol 18:6353–6364. doi:10.1128/MCB.18.11.6353

Braunbeck T, Kais B, Lammer E et al (2015) The fish embryo test (FET): origin, applications, and future. Environ Sci Pollut Res Int 22:16247–16261. doi:10.1007/s11356-014-3814-7

Cambier S, Gonzalez P, Nathalie MD et al (2012) Effects of dietary methylmercury on the zebrafish brain: histological, mitochondrial, and gene transcription analyses. Biometals 25:165–180. doi:10.1007/s10534-011-9494-6

Carney SA, Chen J, Burns CG et al (2006) Aryl hydrocarbon receptor activation produces heart-specific transcriptional and toxic responses in developing zebrafish. Mol Pharmacol 70:549–561. doi:10.1124/mol.106.025304

Chaty S, Rodius F, Vasseur P (2004) A comparative study of the expression of CYP1A and CYP4 genes in aquatic invertebrate (freshwater mussel, Unio tumidus) and vertebrate (rainbow trout, Oncorhynchus mykiss). Aquat Toxicol 69:81–94. doi:10.1016/j.aquatox.2004.04.011

Churchill GA (2004) Using ANOVA to analyze microarray data. BioTechniques 37(173–5):177

Clarkson TW, Magos L (2006) The toxicology of mercury and its chemical compounds. Crit Rev Toxicol 36:609–662. doi:10.1080/10408440600845619

Dalman MR, Deeter A, Nimishakavi G, Duan Z-H (2012) Fold change and p-value cutoffs significantly alter microarray interpretations. BMC bioinformatics 13:S11. doi:10.1186/1471-2105-13-S2-S11

Demir F, Uzun FG, Durak D, Kalender Y (2011) Subacute chlorpyrifos-induced oxidative stress in rat erythrocytes and the protective effects of catechin and quercetin. Pestic Biochem Physiol 99:77–81. doi:10.1016/j.pestbp.2010.11.002

Eisen MB, Spellman PT, Brown PO, Botstein D (1998) Cluster analysis and display of genome-wide expression patterns. Proc Natl Acad Sci 95:14863–14868. doi:10.1073/pnas.95.25.14863

Fedorenkova A, Vonk J (2010) Ecotoxicogenomics: bridging the gap between genes and populations. Environmental science & technology 44:4328–4333

Feiler U, Höss S, Ahlf W et al (2013) Sediment contact tests as a tool for the assessment of sediment quality in German waters. Environ Toxicol Chem 32:144–155. doi:10.1002/etc.2024

Freyhult E, Landfors M, Önskog J et al (2010) Challenges in microarray class discovery: a comprehensive examination of normalization, gene selection and clustering. BMC Bioinformatics 11:1–14. doi:10.1186/1471-2105-11-503

Fujita H, Okimura Y, Utsumi T et al (2006) 4-Hydroxy-3,5,3′,4′-tetrachlorobiphenyl induced membrane permeability transition in isolated rat liver mitochondria. J Clin Biochem Nutr 38:167–175. doi:10.3164/jcbn.38.167

Garcia-Käufer M, Gartiser S, Hafner C et al (2015) Genotoxic and teratogenic effect of freshwater sediment samples from the Rhine and Elbe River (Germany) in zebrafish embryo using a multi-endpoint testing strategy. Environ Sci Pollut Res Int 22:16341–16357. doi:10.1007/s11356-014-3894-4

Giancarlo R, Lo Bosco G, Pinello L (2010) Distance functions, clustering algorithms and microarray data analysis. Lecture notes in computer science. Springer, Berlin Heidelberg, pp 125–138

Hahn ME (2001) Dioxin toxicology and the aryl hydrocarbon receptor: insights from fish and other non-traditional models. Marine biotechnology (New York, NY) 3:S224–S238. doi:10.1007/s10126-001-0045-y

Handley-Goldstone HM, Grow MW, Stegeman JJ (2005) Cardiovascular gene expression profiles of dioxin exposure in zebrafish embryos. Toxicol Sci 85:683–693. doi:10.1093/toxsci/kfi116

Hassan SA, Moussa EA, Abbott LC (2012) The effect of methylmercury exposure on early central nervous system development in the zebrafish (Danio rerio) embryo. J Appl Toxicol 32:707–713. doi:10.1002/jat.1675

Henry T, Spitsbergen J, Hornung MW et al (1997) Early life stage toxicity of 2,3,7,8-tetrachlorodibenzo-p-dioxin in zebrafish (Danio rerio). Toxicol Appl Pharmacol 141:56–68

Ho NY, Yang L, Legradi J et al (2013) Gene responses in the central nervous system of zebrafish embryos exposed to the neurotoxicant methyl mercury. Environmental Science & Technology 47:3316–3325. doi:10.1021/es3050967

Hollert H, Keiter S, König N et al (2003) A new sediment contact assay to assess particle-bound pollutants using zebrafish (Danio rerio) embryos. J Soils Sediments 3:197–207. doi:10.1065/jss2003.09.085

Höss S, Ahlf W, Fahnenstich C et al (2010) Variability of sediment-contact tests in freshwater sediments with low-level anthropogenic contamination-determination of toxicity thresholds. Environ Pollut 158:2999–3010. doi:10.1016/j.envpol.2010.05.013

Howe K, Clark MD, Torroja CF et al (2013) The zebrafish reference genome sequence and its relationship to the human genome. Nature 496:498–503. doi:10.1038/nature12111

Ishida T, Nakajima T, Kudo A, Kawakami A (2010) Phosphorylation of Junb family proteins by the Jun N-terminal kinase supports tissue regeneration in zebrafish. Dev Biol 340:468–479. doi:10.1016/j.ydbio.2010.01.036

Jönsson ME, Jenny MJ, Woodin BR et al (2007) Role of AHR2 in the expression of novel cytochrome P450 1 family genes, cell cycle genes, and morphological defects in developing zebra fish exposed to 3,3′,4,4′,5-pentachlorobiphenyl or 2,3,7,8-tetrachlorodibenzo-p-dioxin. Toxicol Sci 100:180–193. doi:10.1093/toxsci/kfm207

Jönsson ME, Kubota A, Timme-Laragy AR et al (2012) Ahr2-dependence of PCB126 effects on the swim bladder in relation to expression of CYP1 and cox-2 genes in developing zebrafish. Toxicol Appl Pharmacol 265:166–174. doi:10.1016/j.taap.2012.09.023

Keiter S, Peddinghaus S, Feiler U et al (2010) DanTox-a novel joint research project using zebrafish (Danio rerio) to identify specific toxicity and molecular modes of action of sediment-bound pollutants. J Soils Sediments 10:714–717. doi:10.1007/s11368-010-0221-7

Keiter SH, Braunbeck T, Feiler U, et al. (2013) DanTox—Entwicklung und Anwendung eines Verfahrens zur Ermittlung spezifischer Toxizität und molekularer Wirkungsmechanismen sedimentgebundener Umweltschadstoffe mit dem Zebrabärbling (Danio rerio) : Schlussbericht.

Kosmehl T, Otte JC, Yang L et al (2012) A combined DNA-microarray and mechanism-specific toxicity approach with zebrafish embryos to investigate the pollution of river sediments. Reproductive toxicology (Elmsford, NY) 33:245–253. doi:10.1016/j.reprotox.2012.01.005

Kwong TC (2002) Organophosphate pesticides: biochemistry and clinical toxicology. Ther Drug Monit 24:144–149. doi:10.1097/00007691-200202000-00022

Legradi J (2011) Microarray based transcriptomics and the search for biomarker genes in zebrafish. Ruprecht-Karls Universität, Heidelberg

Lettieri T (2006) Recent applications of DNA microarray technology to toxicology and ecotoxicology. Environ Health Perspect 114:4–9. doi:10.1289/ehp.8194

Lewis RS, Noor SM, Fraser FW et al (2014) Regulation of embryonic hematopoiesis by a cytokine-inducible SH2 domain homolog in zebrafish. Journal of immunology (Baltimore, Md : 1950) 192:5739–5748. doi:10.4049/jimmunol.1301376

Li W (2012) Volcano plots in analyzing differential expressions with mRNA microarrays. J Bioinforma Comput Biol 10:1231003. doi:10.1142/S0219720012310038

Liu H, Nie F-H, Lin H-Y et al (2014) Developmental toxicity, oxidative stress, and related gene expression induced by dioxin-like PCB 126 in zebrafish (Danio rerio). Environmental toxicology n/a-n/a. doi:10.1002/tox.22044

Liu L, Xu Y, Xu L et al (2015) Analysis of differentially expressed proteins in zebrafish (Danio rerio) embryos exposed to chlorpyrifos. Comparative biochemistry and physiology Toxicology & pharmacology : CBP 167:183–189. doi:10.1016/j.cbpc.2014.10.006

McCarthy DJ, Smyth GK (2009) Testing significance relative to a fold-change threshold is a TREAT. Bioinformatics (Oxford, England) 25:765–771. doi:10.1093/bioinformatics/btp053

Murtagh F, Legendre P (2014) Ward's hierarchical agglomerative clustering method: which algorithms implement Ward's criterion? J Classif 31:274–295. doi:10.1007/s00357-014-9161-z

Nishihara Y (1985) Comparative study of the effects of biphenyl and Kanechlor-400 on the respiratory and energy linked activities of rat liver mitochondria. Occup Environ Med 42:128–132. doi:10.1136/oem.42.2.128

Nishihara Y, Utsumi K (1987) 4-Chloro-4′-biphenylol as an uncoupler and an inhibitor of mitochondrial oxidative phosphorylation. Biochem Pharmacol 36:3453–3457

Nishihara Y, Robertson LW, Oesch F, Utsumi K (1986) The effects of tetrachlorobiphenyls on the electron transfer reaction of isolated rat liver mitochondria. Life Sci 38:627–635. doi:10.1016/0024-3205(86)90056-1

Pavlidis P (2003) Using ANOVA for gene selection from microarray studies of the nervous system. Methods 31:282–289. doi:10.1016/S1046-2023(03)00157-9

Prochazkova J, Kabatkova M, Bryja V et al (2011) The interplay of the aryl hydrocarbon receptor and beta-catenin alters both AhR-dependent transcription and Wnt/beta-catenin signaling in liver progenitors. Toxicol Sci 122:349–360. doi:10.1093/toxsci/kfr129

Richter CA, Garcia-Reyero N, Martyniuk C et al (2011) Gene expression changes in female zebrafish (Danio rerio) brain in response to acute exposure to methylmercury. Environmental toxicology and chemistry / SETAC 30:301–308. doi:10.1002/etc.409

Salvi M, Toninello A (2001) Aroclor 1254 inhibits the mitochondrial permeability transition and release of cytochrome c: a possible mechanism for its in vivo toxicity. Toxicol Appl Pharmacol 176:92–100. doi:10.1006/taap.2001.9271

Samson JC, Shenker J (2000) The teratogenic effects of methylmercury on early development of the zebrafish, Danio rerio. Aquat Toxicol 48:343–354. doi:10.1016/S0166-445X(99)00044-2

Schiwy S, Bräunig J, Alert H et al (2014) A novel contact assay for testing aryl hydrocarbon receptor (AhR)-mediated toxicity of chemicals and whole sediments in zebrafish (Danio rerio) embryos. Environ Sci Pollut Res Int. doi:10.1007/s11356-014-3185-0

Schlezinger JJ, Struntz WDJ, Goldstone JV, Stegeman JJ (2006) Uncoupling of cytochrome P450 1A and stimulation of reactive oxygen species production by co-planar polychlorinated biphenyl congeners. Aquatic toxicology (Amsterdam, Netherlands) 77:422–432. doi:10.1016/j.aquatox.2006.01.012

Shelton DW, Goeger DE, Hendricks JD, Bailey GS (1986) Mechanisms of anti-carcinogenesis: the distribution and metabolism of aflatoxin B1 in rainbow trout fed aroclor 1254. Carcinogenesis 7:1065–1071. doi:10.1093/carcin/7.7.1065

Silkworth JB, Koganti A, Illouz K et al (2005) Comparison of TCDD and PCB CYP1A induction sensitivities in fresh hepatocytes from

human donors, Sprague-Dawley rats, and rhesus monkeys and HepG2 cells. Toxicol Sci 87:508–519. doi:10.1093/toxsci/kfi261

Smyth GK (2004) Linear models and empirical Bayes methods for assessing differential expression in microarray experiments. Stat Appl Genet Mol Biol 3:1–26. doi:10.2202/1544-6115.1027

Snape JR, Maund SJ, Pickford DB, Hutchinson TH (2004) Ecotoxicogenomics: the challenge of integrating genomics into aquatic and terrestrial ecotoxicology. Aquatic toxicology (Amsterdam, Netherlands) 67:143–154. doi:10.1016/j.aquatox.2003.11.011

Snell TW, Brogdon SE, Morgan MB (2003) Gene expression profiling in ecotoxicology. Ecotoxicology (London, England) 12:475–483

Straus DL, Chambers JE (1995) Inhibition of acetylcholinesterase and aliesterases of fingerling channel catfish by chlorpyrifos, parathion, and S,S,S-tributyl phosphorotrithioate (DEF). Aquat Toxicol 33: 311–324. doi:10.1016/0166-445X(95)00024-X

Uzun FG, Kalender Y (2013) Chlorpyrifos induced hepatotoxic and hematologic changes in rats: the role of quercetin and catechin. Food Chem Toxicol 55:549–556. doi:10.1016/j.fct.2013.01.056

Van Aggelen G, Ankley GT, Baldwin WS et al (2010) Integrating omic technologies into aquatic ecological risk assessment and environmental monitoring: hurdles, achievements, and future outlook. Environ Health Perspect 118:1–5. doi:10.1289/ehp.0900985

Villeneuve D, Volz DC, Embry MR et al (2014a) Investigating alternatives to the fish early-life stage test: a strategy for discovering and annotating adverse outcome pathways for early fish development. Environmental toxicology and chemistry / SETAC 33:158–169. doi: 10.1002/etc.2403

Villeneuve DL, Crump D, Garcia-Reyero N et al (2014b) Adverse outcome pathway (AOP) development I: strategies and principles. Toxicol Sci 142:312–320. doi:10.1093/toxsci/kfu199

Whitney K, Seidler F, Slotkin T (1995) Developmental neurotoxicity of chlorpyrifos: cellular mechanisms. Toxicol Appl Pharmacol 134:53–62

Xiao Y, Hsiao T-H, Suresh U et al (2014) A novel significance score for gene selection and ranking. Bioinformatics (Oxford, England) 30: 801–807. doi:10.1093/bioinformatics/btr671

Yang L, Kemadjou JR, Zinsmeister C et al (2007) Transcriptional profiling reveals barcode-like toxicogenomic responses in the zebrafish embryo. Genome Biol 8:R227. doi:10.1186/gb-2007-8-10-r227

Yang L, Ho NY, Müller F, Strähle U (2010) Methyl mercury suppresses the formation of the tail primordium in developing zebrafish embryos. Toxicol Sci 115:379–390. doi:10.1093/toxsci/kfq053

Yang D, Lauridsen H, Buels K et al (2011) Chlorpyrifos-oxon disrupts zebrafish axonal growth and motor behavior. Toxicol Sci 121:146–159. doi:10.1093/toxsci/kfr028

Yen J, Donerly S, Levin ED, Linney EA (2011) Differential acetylcholinesterase inhibition of chlorpyrifos, diazinon and parathion in larval zebrafish. Neurotoxicol Teratol 33:735–741. doi:10.1016/j.ntt.2011.10.004